Numer Algor (2015) 68:769–790
DOI 10.1007/s11075-014-9871-7

ORIGINAL PAPER

Estimation of unknown boundary functions in an inverse heat conduction problem using a mollified marching scheme

M. Garshasbi · H. Dastour

Received: 20 August 2013 / Accepted: 30 April 2014 / Published online: 15 May 2014

Abstract In this article, a one-dimensional inverse heat conduction problem with unknown nonlinear boundary conditions is studied. In many practical heat transfer situations, the heat transfer coefficient depends on the boundary temperature and the dependence has a complicated or unknown structure. For this reason highly nonlinear boundary conditions are imposed involving both the flux and the temperature. A numerical procedure based on the mollification method and the space marching scheme is developed to solve numerically the proposed inverse problem. The stability and convergence of numerical solutions are investigated and the numerical results are presented and discussed for some test problems.

Keywords Inverse heat conduction · Nonlinear boundary condition · Mollification · Space marching method

1 Introduction

Most of the realistic descriptions of the heat transfer processes in different environments are characterized by a nonlinear relationship between the normal heat flux and the temperature on the boundary. In other words, these problems are described by a partial differential equation subjected to a nonlinear boundary condition [1, 2]. When the temperature level becomes high, radiation and/or change of phase may occur and as a result, the boundary conditions become nonlinear. For instance the problems of heat diffusion with nonlinear boundary conditions appear in combustion systems, where in the pre-ignition heating, the particle entering a furnace and traveling toward

M. Garshasbi (✉) · H Dastour
School of Mathematics, Iran University of Science and Technology, Tehran, Iran
e-mail: m_garshasbi@iust.ac.ir

a flame front receives heat uniformly by thermal radiation from the furnace walls and losses heat uniformly by convection to the surrounding gases [3, 4].

However, there are many practical heat transfer situations at high temperatures, or in hostile environments, e.g. combustion chambers, cooling steel processes, etc. in which either the actual method of heat transfer is not known, or it cannot be assumed that the governing boundary conditions have such a simple form [5].

In recent years, with respect to the variety of application of partial differential equation, an important mathematically challenging and well-investigated class of problems are the identification of coefficients and unknown functions that appear in partial differential equations. The identification of coefficients in heat equations known as inverse heat conduction problems (IHCP's) usually is an ill-posed problem that has received considerable attention from many researchers in a variety of fields, using different methods. Some detailed treatments of problems in these areas can be found in [6-13]. However, the determination of unknown functions and parameters in the boundary conditions is less developed.

It is well-known that the determination of nonlinear boundary conditions is an ill-posed problem. In many problems, even if a unique solution exists, it will not depend continuously on the input data. Therefore using the regularization methods seems necessary in order to stabilize the solution. For such problems one may find many studies in literature. For instance in [7], Cannon and Zachman used the Green's function method to transform some inverse problems to ill-posed operator equations of the first kind. In [8–10], Rosch derived stability estimates for the identification of nonlinear heat transfer laws and investigated numerically the determination of unknown boundary functions as optimal control problems. In [11, 12], the authors employed the boundary element method to approximate the unknown boundary functions. In [13], the authors utilized the conjugate gradient method as an iterative regularization method to approximate unknown boundary functions. Using these methods, according to the author's experience, usually one should deal with the solution of nonlinear system of equations or a large number of simultaneous linear algebraic equations. Furthermore in iterative methods the number of iterations require to achieve a modest accuracy may become large.

In this work the application of the mollification method and the space marching scheme is investigated for solving numerically the inverse problem of identification of nonlinear boundary conditions in heat conduction. Our main purpose of the this paper is to present and analyze a stable method, based on marching mollification techniques, for the numerical computation of boundary functions. The mollification method has been widely used for the stable numerical solution of ill-posed problems based on parabolic equations [14-18]. This is due to the known fact that mollification is a reliable regularization procedure. More recently, it has been proved that mollification is a versatile and useful tool when dealing with parabolic equations and conservation laws [17, 18]. The precise forms of the nonlinear boundary functions are supposed to be unknown and for this reason a numerical approach is adopted in which the unknown boundary functions are approximated by polynomial functions with unknown coefficients to be determined. It should be noted that efficiency, simplicity of implementation and very modest computational costs make the numerical procedures established in this study particularly attractive.

The outline of the present paper is as follows: In Section 2, the mathematical formulation of our interest problem is stated as an inverse problem. A numerical procedure based on the mollification method and the space marching scheme is developed for solving the proposed inverse problem in Section 3. The convergence and stability analysis of solution are established in Section 4. In the last section three test problems are considered and the numerical results are presented for them.

2 Description of the inverse problem

Consider following initial boundary value problem

$$u_t(x,t) - a^2 u_{xx}(x,t) = f(x,t), \quad 0 < x < 1, \ 0 < t < 1, \tag{1}$$
$$u(x,0) = \gamma(x), \quad 0 \le x \le 1, \tag{2}$$
$$u_x(0,t) = G(u(0,t)) + \psi_1(t), \quad 0 \le t \le 1, \tag{3}$$
$$u_x(1,t) = H(u(1,t)) + \psi_2(t), \quad 0 \le t \le 1, \tag{4}$$

where u represents the unknown temperature of the one-dimensional rod $(0, 1)$, $f(x,t)$ show the source (or sink) term, $\gamma(x)$ is the given initial temperature, the functions $G(u)$ and $H(u)$ represent the unknown law for the boundary conditions and $\psi_1(t)$ and $\psi_2(t)$ are known functions of time. It is assumed that $f(x,t)$ and $\gamma(x)$ are L_2 functions, $\psi_1(t)$ and $\psi_2(t)$ are continuous functions and $G(u)$ and $H(u)$ are Lipschitz continuous functions. In addition, the compatibility conditions associated with (2)–(4) require that $\gamma'(0) = G(\gamma(0)) + \psi_1(0)$ and $\gamma'(1) = H(\gamma(1)) + \psi_2(1)$. The existence and uniqueness of solution of direct problem (1)–(4) are investigated in [1, 7].

The unknown boundary functions have to be identified by means of measurements of the temperature u. The measurements can be obtained from some interior temperature sensors at positions x_i; $i = 1, 2, ...S$, in the whole time interval $(0, 1)$ or at discrete times t_j; $j = 1, 2, ...\bar{S}$, [6]. Here it is considered that the measurements of the temperature are available at two interior points x_1 and x_2 in the whole time interval $(0, 1)$. Using these measurements, one can estimates the heat flux at the interior point x_1. The temperature and heat flux at $x = x_1$ $(0 < x_1 < 1)$ are considered as overspecified conditions as follows

$$u(x_1,t) = \varphi_1(t), 0 \le t \le 1, \tag{5}$$
$$u_x(x_1,t) = \varphi_2(t), 0 \le t \le 1. \tag{6}$$

In sequence we will introduce a numerical marching scheme based on the mollification method (see [15, 16]) to find the solution of the problem (1)–(6) under the assumption that $\gamma(x)$, $\psi_1(t)$, $\psi_2(t)$, $\varphi_1(t)$ and $\varphi_2(t)$ are only known approximately as $\gamma^\varepsilon(x)$, $\psi_1^\varepsilon(x)$, $\psi_2^\varepsilon(x)$, $\varphi_1^\varepsilon(t)$ and $\varphi_2^\varepsilon(t)$ such that $\|\gamma(x) - \gamma^\varepsilon(x)\|_\infty \le \varepsilon$, $\|\psi_1(t) - \psi_1^\varepsilon(t)\|_\infty \le \varepsilon$, $\|\psi_2(t) - \psi_2^\varepsilon(t)\|_\infty \le \varepsilon$, $\|\varphi_1(t) - \varphi_1^\varepsilon(t)\|_\infty \le \varepsilon$ and $\|\varphi_2(t) - \varphi_2^\varepsilon(t)\|_\infty \le \varepsilon$. Because of the presence of the noise in the problem's data, we first stablize the problem using the mollification method.

3 Discrete mollification and space marching scheme

3.1 Discrete mollification

Let $\delta > 0$, $p > 0$, $A_p = (\int_{-p}^{p} \exp(-s^2)ds)^{-1}$, $I = [0, 1]$, $Z = \{1, 2, \cdots, M\}$, and $I_\delta = [p\delta, 1 - p\delta]$. Notice that the interval I_δ is nonempty whenever $p < 1/2\delta$.

Furthermore suppose $K = \{x_j : j \in Z\} \subset I$, satisfying

$$x_{j+1} - x_j > d > 0, \, j \in Z, \tag{7}$$

and

$$0 \leq x_1 < x_2 < \cdots < x_M \leq 1, \tag{8}$$

where d is a positive constant. Now if $G = \{g_j\}_{j\in Z}$ be a discrete function defined on K and $s_0 = s_M = 0$ and $s_j = (1/2)(x_j + x_{j+1}), \;\; 1 \leq j \leq M - 1$, then the discrete $\delta-$mollification of G is defined by [14]

$$J_\delta G(x) = \sum_{j=1}^{M} \left(\int_{s_{j-1}}^{s_j} \rho_\delta(x - s)ds \right) g_j, \tag{9}$$

where

$$\rho_{\delta,p}(x) = \begin{cases} A_p \delta^{-1} \exp\left(-\frac{x^2}{\delta^2}\right), & |x| \leq p\delta, \\ 0, & |x| > p\delta. \end{cases} \tag{10}$$

Notice that, $\sum_{j=1}^{M} (\int_{s_{j-1}}^{s_j} \rho_\delta(x - s)ds) = \int_{-p\delta}^{p\delta} \rho_\delta(s)ds = 1$
Let $\Delta x = \sup_{j\in Z}(x_{j+1} - x_j)$, some useful results of the consistency, stability and convergence of discrete δ-mollification are as follows [15-17]

Theorem 1 1. *If $g(x)$ is uniformly Lipschitz in I and $G = \{g_j = g(x_j) : j \in Z\}$ is the discrete version of g, then there exists a constant C, independent of δ, such that*

$$\| J_\delta G - g \|_{\infty, I_\delta} \leq C(\delta + \Delta x). \tag{11}$$

Moreover, if $g'(x) \in C(I)$ then,

$$\| (J_\delta G)' - g' \|_{\infty, I_\delta} \leq C\left(\delta + \frac{\Delta x}{\delta}\right). \tag{12}$$

2. *If the discrete functions $G = \{g_j : j \in Z\}$ and $G^\varepsilon = \{g_j^\varepsilon : j \in Z\}$, which are defined on K, satisfy $\| G - G^\varepsilon \|_{\infty,K} \leq \varepsilon$, then we have*

$$\| J_\delta G - J_\delta G^\varepsilon \|_{\infty, I_\delta} \leq \varepsilon, \tag{13}$$

$$\| (J_\delta G)' - (J_\delta G^\varepsilon)' \|_{\infty, I_\delta} \leq \frac{C\varepsilon}{\delta}. \tag{14}$$

3. *If $g(x)$ is uniformly Lipschitz on I, let $G = \{g_j = g(x_j) : j \in Z\}$ be the discrete version of g and $G^\varepsilon = \{g_j^\varepsilon : j \in Z\}$ be the perturbed discrete version of g satisfying $\| G - G^\varepsilon \|_{\infty,K} \leq \varepsilon$. then,*

$$\| J_\delta G^\varepsilon - J_\delta g \|_{\infty, I_\delta} \leq C(\varepsilon + \Delta x), \tag{15}$$

and

$$\| J_\delta G^\varepsilon - g \|_{\infty, I_\delta} \leq C(\varepsilon + \delta + \Delta x). \tag{16}$$

Moreover, if $g'(x) \in C(I)$ then,

$$\| (J_\delta G^\varepsilon)' - (J_\delta g)' \|_{\infty, I_\delta} \leq \frac{C}{\delta}(\varepsilon + \Delta x), \tag{17}$$

$$\| (J_\delta G^\varepsilon)' - g' \|_{\infty, I_\delta} \leq C\left(\delta + \frac{\varepsilon}{\delta} + \frac{\Delta x}{\delta}\right). \tag{18}$$

Denoting the centered difference operator by $\boldsymbol{D}$, i.e., $\boldsymbol{D} f(x) = \frac{f(x+\Delta x) - f(x-\Delta x)}{2\Delta x}$. Then we have the following results [14]

Theorem 2 1. *If $g' \in C^1(R^1)$, and $G = \{g_j = g(x_j) : j \in Z\}$ is the discrete version of g, with G, G^ε satisfying $\| G - G^\varepsilon \|_{\infty, K} \leq \varepsilon$, then,*

$$\| \boldsymbol{D}(J_\delta G^\varepsilon) - (J_\delta g)' \|_\infty \leq \frac{C}{\delta}(\varepsilon + \Delta x) + C_\delta (\Delta x)^2, \tag{19}$$

$$\| \boldsymbol{D}(J_\delta G^\varepsilon) - g' \|_\infty \leq C\left(\delta + \frac{\varepsilon}{\delta} + \frac{\Delta x}{\delta}\right) + C_\delta (\Delta x)^2. \tag{20}$$

2. *Suppose $G = \{g_j : j \in Z\}$ is a discrete function defined on a set K, and $\boldsymbol{D}_0^\delta$ is a differentiation operator defined by $\boldsymbol{D}_0^\delta(G) = \boldsymbol{D}(J_\delta G)(x)$, then*

$$\| \boldsymbol{D}_0^\delta(G) \|_{\infty, K} \leq \frac{C}{\delta} \| G \|_{\infty, K} . \tag{21}$$

3.2 Numerical implementation of discrete mollification

Computation of $J_\delta g$ throughout a domain such as [0, 1] requires handling of data near the borders. The usual ways are the extension of g to a slightly bigger interval $I'_\delta = [-p\delta, 1 + p\delta]$ or the consideration of the mollified function restricted to the subinterval $I_\delta = [p\delta, 1p\delta]$.

In this regard, different approaches have been proposed in the literature. For instance in [15] an approach based on the techniques for image reconstruction and digital signal processing is described. This technique is modified in [17, 18] as a nonlinear discrete mollifier. Here we follow the strategy introduced in [15]. We try for constant extension g^* of g to the intervals $[-p\delta, 0]$ and $[1, 1 + p\delta]$, satisfying the conditions $||J_\delta g^* - g||_{L^2[0,p\delta]}$ and $||J_\delta g^* - g||_{L^2[1-p\delta,1]}$ are minimum. At the boundary $t = 1$, the unique solution to this optimization problem is given by [15]

$$g^* = \frac{\int_{1-p\delta}^{1} [g^\epsilon(t) - \int_0^1 \rho_\delta(t-s) g(s) ds][\int_1^{1+p\delta} \rho_\delta(t-s)]dt}{\int_{1-p\delta}^{1} [\int_1^{1+p\delta} \rho_\delta(t-s) ds]dt} \tag{22}$$

A similar result con be obtained at the end point $t = 0$.

For each $\delta > 0$, the extended function is defined on the interval I'_δ and the corresponding mollified function is computed on $I = [0, 1]$. All the conclusions and error estimates hold in the subinterval I_δ. Details on the computation of mollified operators and mollification parameters can be found in [15-18].

3.3 Regularized problem and the marching scheme

The regularized problem is formulated as follows

$$v_t(x,t) - a^2 v_{xx}(x,t) = f(x,t), \quad 0 < x < 1, \; 0 < t < 1, \tag{23}$$

$$v(x,0) = J_{\delta'}\gamma(x), \quad 0 \le x \le 1, \tag{24}$$

$$v_x(0,t) = G(v(0,t)) + J_{\delta_1}\psi_1(t), \quad 0 \le t \le 1, \tag{25}$$

$$v_x(1,t) = H(v(1,t)) + J_{\delta_2}\psi_2(t), \quad 0 \le t \le 1. \tag{26}$$

To solve this inverse problem, using the overspecified conditions (5)–(6), first we consider the following auxiliary regulized inverse problem: Determine $v(x,t)$, $v_x(x,t) \in [0,1] \times [0,1]$ satisfying

$$v_t(x,t) - a^2 v_{xx}(x,t) = f(x,t), \quad 0 < x < 1, \; 0 < t < 1, \tag{27}$$

$$v(x,0) = J_{\delta'}\gamma(x), \quad 0 \le x \le 1, \tag{28}$$

$$v(x_1,t) = J_{\delta_0}\varphi_1(t), \quad 0 \le t \le 1, \tag{29}$$

$$v_x(x_1,t) = J_{\delta_0^*}\varphi_2(t), \quad 0 \le t \le 1, \tag{30}$$

where the radii of mollification, δ', δ_1, δ_2, δ_0 and δ_0^* are chosen automatically using the Generalized Cross Validation (GCV) method [15]. The existence and uniqueness of solution of this problem is proved in [13].

Let M and N be positive integers, $h = \Delta x = 1/M$ and $k = \Delta t = 1/N$ be the parameters of the finite differences discretization of $I = [0, 1]$, and $M_1 = [x_1/h]$ ($M_1 \in \{0, 1, 2, \ldots, M\}$). We introduce the following discrete functions

$U_{i,n}$: the discrete computed approximations of $v(ih, nk)$,
$W_{i,n}$: the discrete computed approximations of $v_t(ih, nk)$,
$Q_{i,n}$: the discrete computed approximations of $v_x(ih, nk)$,
$F_{i,n}$: the discrete computed approximations of $f(ih, nk)$.

The algorithm of space marching scheme may be written when $0 < x < x_1$ (the backward case) and when $x_1 < x < 1$ (the forward case) as follows

1. Select $\delta_0 = \delta_{M_1}$, $\delta_0^* = \delta_{M_1}^*$ and δ'.
2. Perform mollification of φ_1^ε, φ_2^ε in the interval [0, 1].
   $U_{M_1,n} = J_{\delta_{M_1}}\varphi_1^\varepsilon(nk)$ $(n \ne 0)$, $\quad U_{i,0} = J_{\delta'}\gamma^\varepsilon(ih)$, $i \in \{0, 1, \ldots, M\}$
   $Q_{M_1,n} = J_{\delta_{M_1}^*}\varphi_2^\varepsilon(nk)$.
3. Perform mollified differentiation in time of $J_{\delta_{M_1}}\varphi_1^\varepsilon(nk)$. Set
   $W_{M_1,n} = \mathbf{D}_t(J_{\delta_{M_1}}\varphi_1^\varepsilon(nk))$ $(n \ne 0)$, $\quad W_{M_1,0} = \mathbf{D}_t(J_{\delta'_{M_1}}\gamma^\varepsilon(M_1 h))$.

4. For the forward case, initialize $i = M_1$. Do while $i \leq M - 1$,

$$U_{i+1,n} = U_{i,n} + hQ_{i,n}, \ (n \neq 0), \tag{31}$$
$$Q_{i+1,n} = Q_{i,n} + \frac{h}{a^2}\left(W_{i,n} - F_{i,n}\right), \tag{32}$$
$$W_{i+1,n} = W_{i,n} + h\mathbf{D}_t(J_{\delta_i^*} Q_{i,n}). \tag{33}$$

5. For the backward case, initialize $i = M_1$. Do while $i \geq 1$,

$$U_{i-1,n} = U_{i,n} - hQ_{i,n}, \ (n \neq 0), \tag{34}$$
$$Q_{i-1,n} = Q_{i,n} - \frac{h}{a^2}\left(W_{i,n} - F_{i,n}\right), \tag{35}$$
$$W_{i-1,n} = W_{i,n} - h\mathbf{D}_t(J_{\delta_i^*} Q_{i,n}). \tag{36}$$

From now on, if $X_{i,n}$ is a discrete function, we denote $|X_i| = \max_n |X_{i,n}|$. We also consider a smoothing assumption to discuss the stability and convergence of the scheme as follows

$$u(x,t) \in C^2(I \times I). \tag{37}$$

4 Stability and convergence analysis

In this section, we analyze the stability and convergence of the forward marching scheme (31)–(33) and the backward marching scheme (34)–(36).

Table 1 Relative l_2 error norms for the IHCP given by Example 1

			Backward Case			Forward Case		
M	N	ε	u	u_t	u_x	u	u_t	u_x
64	64	0.0001	0.016027	0.018359	0.020782	0.016812	0.017623	0.020765
128	128	0.0001	0.0081815	0.010998	0.010414	0.0083846	0.013866	0.010387
256	256	0.0001	0.0041479	0.0089689	0.0052912	0.0042121	0.010788	0.0052184
512	512	0.0001	0.00209	0.005965	0.0026925	0.0021374	0.0087809	0.0029689
64	64	0.001	0.016025	0.030214	0.020893	0.016837	0.044144	0.020918
128	128	0.001	0.0081869	0.027501	0.010309	0.0083926	0.035378	0.010718
256	256	0.001	0.0041353	0.011848	0.005599	0.0041642	0.0099161	0.0054997
512	512	0.001	0.0022839	0.017451	0.0038994	0.0021011	0.0064247	0.0027941
64	64	0.01	0.015974	0.051993	0.021299	0.017518	0.068423	0.021183
128	128	0.01	0.0086671	0.03394	0.011564	0.0089155	0.034436	0.011565
256	256	0.01	0.0053385	0.056553	0.010614	0.0057859	0.020754	0.0081614
512	512	0.01	0.0039662	0.095607	0.009806	0.0036231	0.015102	0.0045945

Theorem 3 *For the forward marching scheme* (31)–(33)*, there exists a constant* Λ_1*, such that*

$$\max\{|U_M|, |Q_M|, |W_M|, M_f\} \leq \Lambda_1 \max\{|U_{M_1}|, |Q_{M_1}|, |W_{M_1}|, M_f\}, \tag{38}$$

and for the backward marching scheme (34)–(36)*, there exists a constant* Λ_2*, such that*

$$\max\{|U_0|, |Q_0|, |W_0|, M_f\} \leq \Lambda_2 \max\{|U_{M_1}|, |Q_{M_1}|, |W_{M_1}|, M_f\}. \tag{39}$$

Proof Here the first inequality for the forward case is proved. The second inequality may be derived similarly. Let $|\delta|_{-\infty} = \min_i(\delta_i, \delta_i^*, \delta_i')$ and $M_f = \max_{(x,t)\in[0,1]\times[0,1]}\{|f(x,t)|\}$. Applying Theorem 2 yields

$$|\mathbf{D}_t(Q_{i,n})| \leq \frac{C}{|\delta|_{-\infty}}|Q_{i,n}|, \tag{40}$$

where C is a constant. Now by using (33) and (40) we have

$$|W_{i+1,n}| \leq \left(1 + h\frac{C}{|\delta|_{-\infty}}\right)\max\{|Q_{i,n}|, |W_{i,n}|\}. \tag{41}$$

Also from (31) and (32) we have

$$|U_{i+1,n}| \leq (1+h)\max\{|U_{i,n}|, |Q_{i,n}|\}, \tag{42}$$

$$|Q_{i+1,n}| \leq \left(1 + \frac{h}{a^2}\right)\max\{|Q_{i,n}|, |W_{i,n}|, M_f\}. \tag{43}$$

Let $C_\delta = \max\left\{1, \frac{1}{a^2}, \frac{C}{|\delta|_{-\infty}}\right\}$, from (41)–(42) we obtain

$$\max\{|U_{i+1}|, |Q_{i+1}|, |W_{i+1}|, M_f\} \leq (1 + hC_\delta)\max\{|U_i|, |Q_i|, |W_i|, M_f\},$$

and iterating this last inequality $L = M - M_1$ times, we have

$$\max\{|U_M|, |Q_M|, |W_M|, M_f\} \leq (1 + hC_\delta)^L \max\{|U_{M_1}|, |Q_{M_1}|, |W_{M_1}|, M_f\},$$

which implies

$$\max\{|U_M|, |Q_M|, |W_M|, M_f\} \leq \exp(C_\delta)\max\{|U_{M_1}|, |Q_{M_1}|, |W_{M_1}|, M_f\}.$$

Letting $\Lambda_1 = \exp(C_\delta)$ completed the proof of this statement. □

Theorem 4 *For the forward and backward marching schemes* (31)–(33) *and* (34)–(36)*, for fixed* δ *as* h*,* k *and* ε *tend to zero, the discrete mollified solution converges to the mollified exact solution restricted to the grid points.*

Proof Here we prove the convergence of the forward case. The convergence of the backward scheme yields similarly. From the definitions of discrete error functions, let

Table 2 The RMS-norm errors between the computed and the exact boundary functions G and H for the IHCP given by Example 1

$M = N$ ε	K	1	2	3	4	5	6	7	8
64	G_k	0.11355	0.057522	0.057601	0.059144	0.062237	0.064666	0.066637	0.068153
0.0001	H_k	0.10232	0.10232	0.10211	0.10197	0.10179	0.10169	0.10156	0.10151
128	G_k	0.080633	0.023356	0.022989	0.022618	0.022589	0.022761	0.02309	0.023308
0.0001	H_k	0.035698	0.0357	0.035663	0.035661	0.035621	0.035618	0.035584	0.03558
256	G_k	0.057145	0.010912	0.0085324	0.0085636	0.0084735	0.008401	0.00834	0.0083163
0.0001	H_k	0.012785	0.012827	0.012835	0.012863	0.012876	0.01292	0.012931	0.012976
512	G_k	0.040337	0.006575	0.0031953	0.0031917	0.003258	0.0032148	0.0032585	0.003226
0.0001	H_k	0.0048848	0.0052031	0.0052313	0.0055535	0.0055847	0.0059389	0.0059949	0.0063163
64	G_k	0.11452	0.062038	0.062003	0.062348	0.067212	0.068581	0.076065	0.076223
0.001	H_k	0.099974	0.10012	0.099608	0.10028	0.099872	0.10025	0.09993	0.099961
128	G_k	0.079614	0.026957	0.029336	0.02826	0.028367	0.028575	0.028693	0.030271
0.001	H_k	0.03432	0.034372	0.034981	0.034958	0.035555	0.035615	0.035975	0.036188
256	G_k	0.056878	0.01115	0.0082421	0.0083799	0.0085189	0.0089741	0.0091166	0.0092003
0.001	H_k	0.012231	0.012465	0.01267	0.012955	0.013099	0.013773	0.013805	0.014803
512	G_k	0.040342	0.0064722	0.0026441	0.0027345	0.0028311	0.0030443	0.0031136	0.0032129
0.001	H_k	0.0053694	0.0061462	0.0064744	0.0071687	0.0072059	0.0072568	0.007235	0.0070916
64	G_k	0.1137	0.043064	0.044237	0.049479	0.049692	0.049663	0.050169	0.053839
0.01	H_k	0.11262	0.11476	0.11399	0.11352	0.11267	0.11225	0.11063	0.11082
128	G_k	0.080657	0.028678	0.029496	0.028755	0.028687	0.02893	0.028904	0.029194
0.01	H_k	0.033708	0.033711	0.033799	0.034201	0.03434	0.034688	0.035021	0.03516
256	G_k	0.056499	0.012366	0.0088885	0.0097291	0.010153	0.011429	0.013503	0.013863
0.01	H_k	0.014342	0.015611	0.015623	0.01587	0.016295	0.016259	0.016737	0.016797
512	G_k	0.040267	0.0085484	0.006471	0.006582	0.0070334	0.0068523	0.0066936	0.0072813
0.01	H_k	0.0062129	0.007756	0.0080824	0.0084686	0.0085547	0.008418	0.009559	0.0094984

Table 3 The coefficients a_j of the function $G(u) \simeq G_K(u) = \sum_{j=0}^{K} a_j u^{K-j}$ for Example 1

K	1	2	3	4	5	6	7	8
a_0	0.33464	2.8052	2.9069	0.27585	5.3526	−22.5096	56.3167	−1234.8305
a_1	−0.59803	−3.3621	−3.0065	2.1676	−17.7164	96.383	−288.8251	6744.5713
a_2	–	0.52636	0.33732	−2.287	25.7705	−168.0696	627.1084	−15908.6813
a_3	–	–	−0.21982	0.036682	−17.367	155.4503	−745.3833	21158.5443
a_4	–	–	–	−0.1744	4.723	−78.9089	525.3908	−17349.4315
a_5	–	–	–	–	−0.74063	19.9484	−218.4712	8981.0536
a_6	–	–	–	–	–	−2.2741	48.6368	−2865.4322
a_7	–	–	–	–	–	–	−4.7524	514.1935
a_8	–	–	–	–	–	–	–	-39.9711

Table 4 The coefficients b_j of the function $H(u) \simeq H_K(u) = \sum_{j=0}^{K} b_j u^{K-j}$ for Example 1

K	1	2	3	4	5	6	7	8
b_0	1.0019	0.012298	−0.012289	0.05938	−0.045578	0.23198	−0.16952	0.73674
b_1	0.0069653	0.95289	0.086667	−0.49403	0.52309	−2.8839	2.6554	−12.22
b_2	–	0.052118	0.8096	1.506	−2.3352	14.7065	−17.4843	87.6513
b_3	–	–	0.1396	−0.98544	5.0665	−39.3478	62.7248	−354.9403
b_4	–	–	–	0.96044	−4.3345	58.2132	−132.3863	887.1334
b_5	–	–	–	–	2.1853	−44.1199	164.3522	−1400.8157
b_6	–	–	–	–	–	14.3111	−110.1031	1364.1842
b_7	–	–	–	–	–	–	31.5509	−747.8782
b_8	–	–	–	–	–	–	–	177.3853

$$\Delta U_{i,n} = U_{i,n} - v(ih, nk), \quad \Delta Q_{i,n} = Q_{i,n} - v_x(ih, nk), \quad \Delta W_{i,n} = W_{i,n} - v_t(ih, nk).$$

Using Taylor series, we obtain some useful equations satisfied by the mollified solution v, namely,

$$\begin{aligned} v((i+1)h, nk) &= v(ih, nk) + hv_x(ih, nk) + O(h^2), \\ v_x((i+1)h, nk) &= v_x(ih, nk) + \frac{h}{a^2}\left(v_t(ih, nk) - f(ih, nk)\right) + O(h^2), \\ v_t((i+1)h, nk) &= v_t(ih, nk) + h\left(\frac{d}{dt}v_x(ih, nk)\right) + O(h^2). \end{aligned}$$

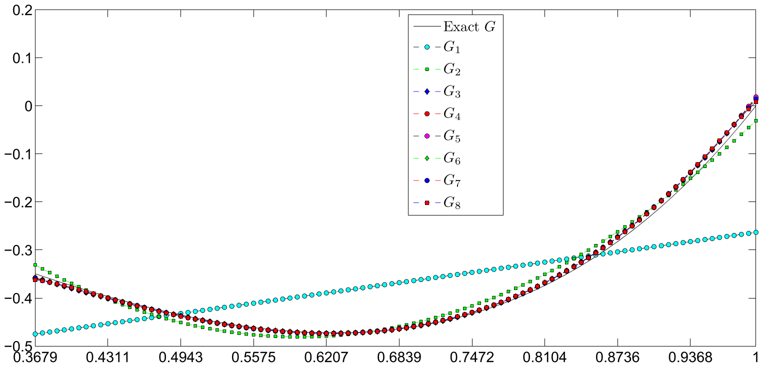

Fig. 1 The analytical and numerical solutions for the boundary function $G(u)$ for the IHCP given by Example 1

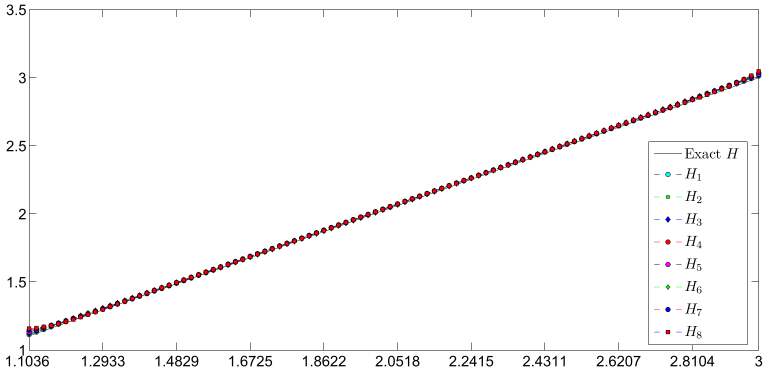

Fig. 2 The analytical and numerical solutions for the boundary function $H(u)$ for the IHCP given by Example 1

On the other hand, one may write

$$\begin{aligned}\Delta U_{i+1,n} &= \Delta U_{i,n} + (U_{i+1,n} - U_{i,n}) - (v((i+1)h, nk) - v(ih, nk)) \\ &= \Delta U_{i,n} + h\Delta Q_{i,n} + O(h^2),\end{aligned} \tag{44}$$

$$\begin{aligned}\Delta Q_{i+1,n} &= \Delta Q_{i,n} + (Q_{i+1,n} - Q_{i,n}) - (v_x((i+1)h, nk) - v_x(ih, nk)) \\ &= \Delta Q_{i,n} + \frac{h}{a^2}\Delta W_{i,n} + O(h^2),\end{aligned} \tag{45}$$

$$\begin{aligned}\Delta W_{i+1,n} &= \Delta W_{i,n} + (W_{i+1,n} - W_{i,n}) - (v_t((i+1)h, nk) - v_t(ih, nk)) \\ &= \Delta W_{i,n} + h(\mathbf{D}_t(J_{\delta_i^*} Q_{i,n}) - v_{xt}(ih, nk)) + O(h^2).\end{aligned} \tag{46}$$

Table 5 Relative l_2 error norms for the IHCP given by Example 2

			Backward Case			Forward Case		
M	N	ε	u	u_t	u_x	u	u_t	u_x
64	64	0.0001	0.0087446	0.068484	0.025957	0.0066747	0.014687	0.024013
128	128	0.0001	0.0022134	0.016669	0.0084626	0.0015356	0.0095322	0.007637
256	256	0.0001	0.0016344	0.010641	0.0053095	0.0011785	0.0067696	0.0049338
512	512	0.0001	0.0014302	0.018803	0.0038801	0.0010641	0.0042677	0.0036166
64	64	0.001	0.0086002	0.13035	0.02631	0.0066426	0.051252	0.024691
128	128	0.001	0.0023625	0.019731	0.0079428	0.0016294	0.014727	0.0080066
256	256	0.001	0.0020292	0.022951	0.0047831	0.0012216	0.014843	0.0052795
512	512	0.001	0.0019211	0.0098536	0.0030316	0.001138	0.011975	0.0040833
64	64	0.01	0.01057	0.053051	0.021717	0.0087537	0.054761	0.028153
128	128	0.01	0.0051014	0.04219	0.0070481	0.0038603	0.045427	0.01253
256	256	0.01	0.0033785	0.085317	0.0051648	0.0026201	0.029708	0.0085531
512	512	0.01	0.0039452	0.23022	0.006241	0.0017832	0.017943	0.0060784

Now from equalities (44)–(46), using the error estimates of discrete mollification from Theorem 2 we have

$$
\begin{aligned}
|\Delta U_{i+1,n}| &\leq |\Delta U_{i,n}| + h|\Delta Q_{i,n}| + O(h^2),\\
|\Delta Q_{i+1,n}| &\leq |\Delta Q_{i,n}| + \frac{h}{a^2}|\Delta W_{i,n}| + O(h^2)\\
|\Delta W_{i+1,n}| &\leq |\Delta W_{i,n}| + h\left(C\frac{|\Delta Q_{i,n}| + k}{|\delta|_{-\infty}} + C_{\delta^*}k^2\right) + O(h^2).
\end{aligned}
$$

Suppose

$$
\Delta_i = \max\{|\Delta U_{i,n}|, |\Delta W_{i,n}|, |\Delta Q_{i,n}|\},\ C_0 = \max\left\{1, \frac{1}{a^2}, \frac{C}{|\delta|_{-\infty}}\right\},\ C_1 = \frac{ck}{|\delta|_{-\infty}} + C_{\delta^*}k^2. \quad (47)
$$

Then we obtain

$$
\Delta_{i+1} \leq (1 + hC_0)\Delta_i + hC_1 + O(h^2) \leq (1 + hC_0)(\Delta_i + C_1) + O(h^2), \quad (48)
$$

Table 6 The RMS-norm errors between the computed and the exact boundary functions G and H for the IHCP given by Example 2

$M = N$ ε	K	1	2	3	4	5	6
64	G_k	0.026568	0.01978	0.019999	0.020106	0.02015	0.020179
0.0001	H_k	0.021001	0.020984	0.021156	0.021446	0.021713	0.021789
128	G_k	0.017064	0.0068626	0.0068875	0.0069002	0.0069067	0.0069103
0.0001	H_k	0.0043505	0.0044436	0.0044434	0.0044441	0.0044427	0.0044368
256	G_k	0.012174	0.0024982	0.0025138	0.0025137	0.0025191	0.0025189
0.0001	H_k	0.0018895	0.0019649	0.0019616	0.0019671	0.0019686	0.0019674
512	G_k	0.0087666	0.00091455	0.00093377	0.00093513	0.00094135	0.0009411
0.0001	H_k	0.00097526	0.0010088	0.0010107	0.0010113	0.0010118	0.0010127
64	G_k	0.026594	0.02028	0.02039	0.020572	0.020585	0.020639
0.001	H_k	0.020985	0.020954	0.02076	0.021191	0.021115	0.021163
128	G_k	0.017171	0.0065618	0.0065985	0.0066075	0.0066329	0.006634
0.001	H_k	0.0041409	0.0042992	0.0042988	0.0043284	0.0043992	0.0044635
256	G_k	0.012274	0.0022328	0.0022751	0.002276	0.0023024	0.0023138
0.001	H_k	0.0019457	0.0020441	0.0020575	0.0021047	0.0021747	0.002246
512	G_k	0.0088433	0.00078561	0.00083135	0.00084304	0.00088251	0.00091965
0.001	H_k	0.00094839	0.0010912	0.0011308	0.0011951	0.0013154	0.0014557
64	G_k	0.026896	0.01705	0.017019	0.017003	0.017446	0.0175
0.01	H_k	0.020899	0.020963	0.021064	0.020897	0.023505	0.023473
128	G_k	0.017435	0.0053519	0.0054839	0.0055712	0.0055803	0.0057199
0.01	H_k	0.0042286	0.0046001	0.0051943	0.0051946	0.0056167	0.0056961
256	G_k	0.012554	0.001955	0.0019761	0.0019949	0.0020508	0.0023352
0.01	H_k	0.0015024	0.00182	0.0018546	0.0019774	0.002225	0.0024216
512	G_k	0.0090422	0.00076111	0.00088195	0.0011646	0.0011809	0.0013363
0.01	H_k	0.001155	0.0012728	0.0013351	0.0020584	0.001843	0.0016649

Table 7 The coefficients a_j of the function $G(u) \simeq G_K(u) = \sum_{j=0}^{K} a_j u^{K-j}$ for Example 2

K	1	2	3	4	5	6
a_0	2.0345	1.0035	0.086192	0.16087	5.4242	5.0898
a_1	−0.56454	0.49109	0.80653	−0.40196	−20.364	−17.6513
a_2	–	0.0026179	0.63752	1.3526	30.2615	22.7687
a_3	–	–	−0.032711	0.37084	−21.2435	−12.2714
a_4	–	–	–	0.015224	8.5807	2.0858
a_5	–	–	–	–	−1.161	1.8336
a_6	–	–	–	–	–	−0.35732

and after $L = M - M_1$ iterations

$$\Delta_L \leq \exp(C_0)(\Delta_{M_1} + C_1). \tag{49}$$

Moreover from

$$\begin{aligned} |\Delta U_{M_1,n}| &\leq C(\varepsilon + k), \\ |\Delta Q_{M_1,n}| &\leq C(\varepsilon + k), \\ |\Delta W_{M_1,n}| &\leq \frac{C}{|\delta|_{-\infty}}(\varepsilon + k) + C_\delta k^2, \end{aligned}$$

we see that when ε, h, and k tend to 0, Δ_{M_1} and C_1 tend to 0. Consequently $(\Delta_0 + C_1)$ tends to 0 and so does Δ_L and this complete the proof of this theorem. □

Corollary 1 *For the boundary functions G and H in the regulized problem* (23)–(26)*, using the numerical results of auxiliary problem* (27)–(30) *yield that as h, k and ε tend to zero, $\Delta G_{0,n}$ and $\Delta H_{1,n}$ tend to zero, where*

$$\Delta G_{0,n} = G(v(0, t_n)) - G(v_{0,n}), \quad \Delta H_{1,n} = H(v(1, t_n)) - H(v_{M,n}). \tag{50}$$

Proof For the boundary function H from (26) we have

$$\begin{aligned} |\Delta H_{1,n}| &= |(v_x(1, nk) - Q_{M,n}) - (J_{\delta_2}\psi_2(nk) - J_{\delta_2}\psi_2^{\varepsilon}(nk))| \\ &\leq |v_x(1, nk) - Q_{M,n}| + |J_{\delta_2}\psi_2(nk) - J_{\delta_2}\psi_2^{\varepsilon}(nk)|. \end{aligned} \tag{51}$$

Table 8 The coefficients b_j of the function $H(u) \simeq H_K(u) = \sum_{j=0}^{K} b_j u^{K-j}$ for Example 2

K	1	2	3	4	5	6
b_0	−0.67048	0.3462	0.22131	21.7783	429.6952	−2371.2762
b_1	0.93737	−0.96396	0.06685	−36.3106	−877.5902	6379.0583
b_2	–	0.99861	−0.84744	22.9091	713.1875	−7073.7371
b_3	–	–	0.98255	−7.1563	−287.9296	4141.8443
b_4	–	–	–	1.6319	56.9949	−1351.0518
b_5	–	–	–	–	−3.6386	232.1254
b_6	–	–	–	–	–	−15.6126

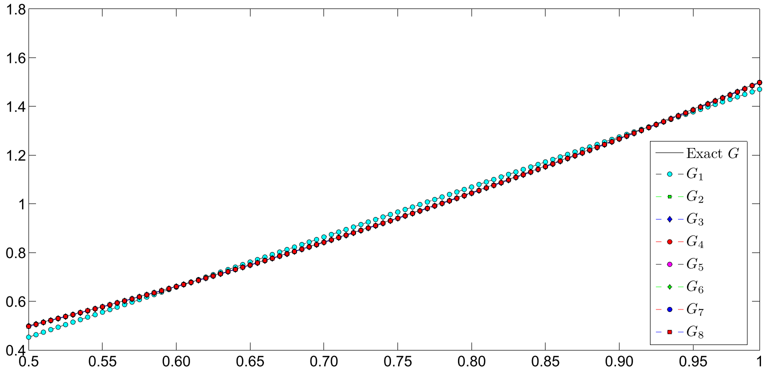

Fig. 3 The analytical and numerical solutions for the boundary function $G(u)$ for the IHCP given by Example 2

Using the results of Theorems 1 and 5, one may see that there exist a constant B such that

$$|\Delta H_{1,n}| \leq \exp(C_0)(\Delta_{M_1} + C_1) + B(\varepsilon + k). \tag{52}$$

This implies that when ε, h, and k tend to zero, $|\Delta H_{1,n}|$ tends to zero too. Similar result can be derived for the boundary function G. □

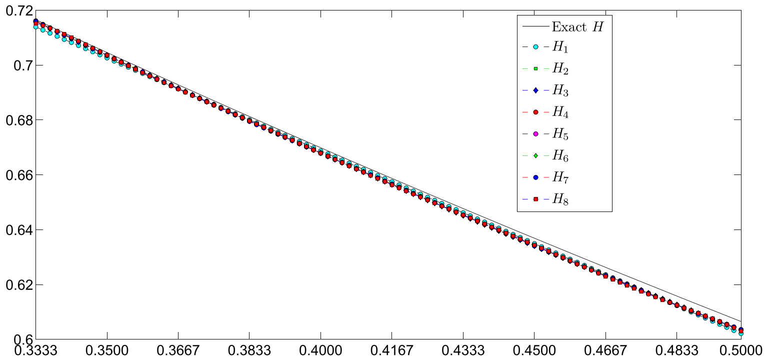

Fig. 4 The analytical and numerical solutions for the boundary function $H(u)$ for the IHCP given by Example 2

5 Numerical results and discussion

To solve the inverse problem of determining the solution (u, G, H), we try to approximate the functions G and H by a polynomial of degree $\leq K$ as follows

$$P_K = \{\sum_{i=0}^{K} a_i u^{K-i},\ a_i \in \mathbf{R}\}, \tag{53}$$

where K maybe considered arbitrary. This assumption reduces the function estimation (infinite dimensional) to a parameter estimation (finite dimensional), also aims to improve the stability of the numerical approximate solution. Using the boundary condition (25) one may see that

$$G(v_{0,n}) = Q_{0,n} - J_{\delta_1}\psi_1^{\varepsilon}(nk),\ n = 0, 1, 2, \cdots, N. \tag{54}$$

To approximate the unknown function G, we deal with a common curve fitting problem as: Determine the polynomial approximation of the unknown function G where its values are known at $N + 1$ points. The unknown polynomial coefficients $a_i, i = 0, 1, \cdots, K$ may be determined using least squares optimization techniques. These coefficients have been calculated by MATLAB software. Similar results may be derived for the function H using mollified solution $v_{M,n}$ and $Q_{M,n}$. In this section, we present some numerical results. In all cases, without loss of generality, we set $p = 3$ (see [15,16]). The radii of mollification are always chosen automatically using the mollification and GCV methods.

Table 9 Relative l_2 error norms for the IHCP given by Example 3

			Backward Case			Forward Case		
M	N	ε	u	u_t	u_x	u	u_t	u_x
64	64	0.0001	0.0081863	0.022012	0.020366	0.0045932	0.00159	0.015838
128	128	0.0001	0.0020098	0.0062643	0.0047161	0.001093	0.0010868	0.0027871
256	256	0.0001	0.0014906	0.0079449	0.0051378	0.00080125	0.0022092	0.0030478
512	512	0.0001	0.001452	0.0074564	0.0049373	0.00081167	0.002297	0.0031131
64	64	0.001	0.0083708	0.035896	0.0213	0.0046069	0.021082	0.016526
128	128	0.001	0.001925	0.016141	0.0044302	0.0023407	0.081811	0.022102
256	256	0.001	0.0015011	0.0078513	0.0054683	0.0012772	0.014151	0.0069964
512	512	0.001	0.0015409	0.01188	0.0068259	0.0012761	0.014725	0.0072605
64	64	0.01	0.0088357	0.048363	0.024418	0.006287	0.061641	0.03245
128	128	0.01	0.002114	0.027392	0.0076254	0.0035297	0.07613	0.028822
256	256	0.01	0.0018593	0.015476	0.0091008	0.0023591	0.039798	0.016102
512	512	0.01	0.0020424	0.032789	0.0149	0.0025049	0.03875	0.016097

Discretized measured approximations of boundary data are modeled by adding random errors to the exact data functions. For example, for the boundary data function $h(x,t)$, its discrete noisy version is generated by [15]

$$h^{\varepsilon}_{j,n} = h(x_j, t_n) + \varepsilon_{j,n}, \qquad j = 0, 1, \ldots, N, n = 0, 1, \ldots, T, \tag{55}$$

where the $(\varepsilon_{j,n})$'s are Gaussian random variables with variance ε^2.

To evaluate the errors for the marching scheme we use the following relative weighted l_2-norm

$$E = \frac{\left[(1/(M+1)(N+1))\Sigma_{i=0}^{M}\ \Sigma_{j=0}^{N}|v(ih, jl) - U_{i,j}|^2\right]^{1/2}}{\left[(1/(M+1)(N+1))\Sigma_{i=0}^{M}\ \Sigma_{j=0}^{N}|v(ih, jl)|^2\right]^{1/2}}, \tag{56}$$

and to evaluate the function specification error we use following RMS-norm

$$R = \sqrt{\frac{1}{N}\Big((w_1 - W_1)^2 + (w_2 - W_2)^2 + \ldots + (w_N - W_N)^2\Big)}, \tag{57}$$

where w_i and W_i respectively represent the exact and computed solutions.

Example 1 In general with the presence of radiation, the heat flux on a surface is the sum of two terms corresponding to convection and surface radiation [2, 4]. As the first example we examine an interesting and important nonlinear IHCP in which the relation between the heat flux and temperature at the boundaries, from a physical point of view, is a fourth-order power in the temperature representing radiative boundary conditions. We investigate the nonlinear IHCP (1)–(6) with the following assumptions

$$\begin{aligned}
x_1 &= 0.5,\ \varphi_1(t) = e^{-t},\ \varphi_2(t) = \pi e^{-t},\ \gamma(x) = 2 - \sin(\pi x) - \cos(\pi x),\ a = 1\\
f(x,t) &= e^{-t}(\cos(\pi x) + \sin(\pi x) - 2) - e^{-t}(\pi^2\cos(\pi x) + \pi^2 sin(\pi x)),\\
\psi_1(t) &= e^{-t} - e^{-4t} - \pi e^{-t},\\
\psi_2(t) &= e^{-t}(\pi - 3).
\end{aligned}$$

The exact solutions for $u(x,t)$, $G(u)$ and $H(u)$ may be derived as

$$u(x,t) = e^{-t}\left(2 - \cos(\pi x) - \sin(\pi x)\right),\ G(u) = u^4 - u,\ H(u) = u.$$

Table 1 displays the relative l_2 errors for computing u, u_t, u_x at three noise levels $\varepsilon = 0.01,\ 0.001,\ 0.0001$ for $N = M = 64,\ 128,\ 256,\ 512$. It can be clearlyobserved that at different noise levels, the relative l_2 errors decreased gradually by increasing the mesh points in both backward and forward cases.

Table 2 illustrates the RMS-norm errors between the computed and the exact boundary functions G and H when $K = 1, 2, ..., 8$, $\varepsilon = 0.0001,\ 0.001,\ 0.01$ and $M = N = 64,\ 128,\ 256,\ 512$. The polynomials are scaled to increase the accuracy. The coefficients a_j and b_j of the functions $G(u) \simeq G_K(u) = \sum_{j=0}^{K} a_j u^{K-j}$ and $H(u) \simeq H_K(u) = \sum_{j=0}^{K} b_j u^{K-j}$ are tabulated in Tables 3 and 4 when $M = N = 512$ and $\varepsilon = 0.0001$. Furthermore, Figs. 1 and 2 show the comparison between the exact and the computed solutions for both functions $G(u)$ and $H(u)$ ($M = N = 512$ and $\varepsilon = 0.0001$). Generally the numerical results demonstrate that at fix noise levels, decreasing the size of h increases the accuracy of the numerical results.

Table 10 The RMS-norm errors between the computed and the exact boundary functions G and H for the IHCP given by Example 3

$M = N$ ε	K	1	2	3	4	5	6	7	8
64	G_k	0.13319	0.078217	0.059943	0.062005	0.056257	0.047769	0.04543	0.045433
0.0001	H_k	0.36496	0.095707	0.095812	0.053323	0.053521	0.041231	0.042215	0.036212
128	G_k	0.091844	0.048243	0.026861	0.026234	0.021563	0.01824	0.017191	0.01455
0.0001	H_k	0.25771	0.064457	0.064541	0.032405	0.032551	0.021056	0.021368	0.015146
256	G_k	0.06547	0.035162	0.022657	0.022956	0.01848	0.020535	0.018436	0.016051
0.0001	H_k	0.18225	0.045663	0.045937	0.023243	0.023493	0.016703	0.018235	0.013075
512	G_k	0.046417	0.025313	0.016774	0.018383	0.014109	0.01704	0.014582	0.013701
0.0001	H_k	0.12888	0.032318	0.032556	0.016483	0.016682	0.012317	0.013575	0.0097627
64	G_k	0.13342	0.077586	0.061276	0.062029	0.056935	0.049887	0.047371	0.047557
0.001	H_k	0.36501	0.096317	0.096351	0.053841	0.054002	0.042546	0.043555	0.037129
128	G_k	0.092647	0.049888	0.033408	0.033491	0.028503	0.032378	0.0315	0.025043
0.001	H_k	0.25772	0.064648	0.065034	0.032953	0.033442	0.024218	0.026159	0.019125
256	G_k	0.065142	0.034486	0.020253	0.019919	0.016186	0.015026	0.01389	0.011558
0.001	H_k	0.18225	0.045588	0.045711	0.023034	0.023211	0.015434	0.016254	0.011589
512	G_k	0.046448	0.025395	0.016935	0.01864	0.014281	0.017262	0.014837	0.013664
0.001	H_k	0.12888	0.032326	0.032589	0.016523	0.016739	0.012441	0.013784	0.0098783
64	G_k	0.15099	0.11384	0.13595	0.19077	0.18491	0.37333	0.38234	0.57905
0.01	H_k	0.36496	0.09471	0.099403	0.063204	0.064316	0.065097	0.069464	0.059262
128	G_k	0.10865	0.076226	0.10989	0.13248	0.16576	0.27527	0.35395	0.44854
0.01	H_k	0.25779	0.066878	0.068755	0.041944	0.043123	0.051713	0.055024	0.049349
256	G_k	0.068558	0.042059	0.039409	0.052784	0.04105	0.072254	0.079674	0.079012
0.01	H_k	0.18227	0.046582	0.047743	0.026124	0.026631	0.027146	0.032691	0.024178
512	G_k	0.048571	0.030853	0.028864	0.040284	0.031065	0.051822	0.058042	0.057986
0.01	H_k	0.12889	0.033145	0.034099	0.018652	0.019334	0.020077	0.024592	0.017754

Since the functions G and H are analytically quartic and linear, we expect the degree of these functions to be $K = 4$ and $K = 1$ respectively to give accurate approximations. Although the values of the approximations of a_k and b_k, when $K = 1, 2..., 8$ deviate significantly from their analytical values, we still obtain good approximations for the boundary functions. This can be explained by the fact that a higher-order function with a variety of coefficients can still be used to approximate with a reasonable accuracy a quartic or a linear function [11].

Example 2 Consider the problem (1)–(6) with the following assumptions

$$x_1 = 0.4,\ \varphi_1(t) = \frac{1}{t^2 + \frac{29}{25}},\ \varphi_2(t) = -\frac{4}{5\left(t^2 + \frac{29}{25}\right)^2},\ \gamma(x) = \frac{1}{x^2+1},\ a = 2$$

$$f(x,t) = -\frac{2t + x^2\ (2t+24) - 8t^2 + 2t^3 - 8}{\left(t^2 + x^2 + 1\right)^3},$$

$$\psi_1(t) = -\frac{t^2+3}{2\left(t^2+1\right)^2},\ \psi_2(t) = -\mathrm{e}^{-\frac{1}{t^2+2}} - \frac{2}{\left(t^2+2\right)^2}.$$

The exact solutions for $u(x,t)$, $G(u)$ and $H(u)$ may be derived as

$$u(x,t) = \frac{1}{t^2 + x^2 + 1},\ G(u) = u^2 + \frac{1}{2}u,\ H(u) = \mathrm{e}^{-u}.$$

The relative l_2 errors for computing u, u_t, u_x in three noise levels when $M = N = 64,\ 128,\ 256,\ 512$, are shown in Table 5. Table 6 illustrates the RMS-norm errors between the computed and the exact boundary functions G and H when the degree K of the functions $G_K(u)$ and $H_K(u)$ increases gradually from 1 to 6 and $\varepsilon = 0.0001,\ 0.001,\ 0.01$ and $M = N = 64,\ 128,\ 256,\ 512$. The numerical results obtained for the coefficients a_j, b_j tabulated in Tables 7 and 8

Table 11 The coefficients a_j of the function $G(u) \simeq G_K(u) = \sum_{j=0}^{K} a_j u^{K-j}$ for Example 3

K	1	2	3	4	5	6	7	8
a_0	−0.31999	−0.28581	0.31406	−0.10023	−0.31414	0.64676	−0.088708	−2.0807
a_1	0.25112	0.25019	−1.2252	0.71387	1.4664	−4.1845	1.266	16.5075
a_2	–	0.062432	0.99766	−1.7371	−2.0619	10.2351	−5.8938	−52.7717
a_3	–	–	−0.060208	1.2234	0.33436	−11.3778	12.6002	86.4005
a_4	–	–	–	−0.082247	0.63704	4.9654	−13.0897	−75.7549
a_5	–	–	–	–	−0.044292	−0.27942	5.5775	33.7685
a_6	–	–	–	–	–	−0.0020517	−0.36899	−7.0989
a_7	–	–	–	–	–	–	0.0010371	1.0592
a_8	–	–	–	–	–	–	–	−0.037167

Table 12 The coefficients b_j of the function $H(u) \simeq H_K(u) = \sum_{j=0}^{K} b_j u^{K-j}$ for Example 3

K	1	2	3	4	5	6	7	8
b_0	−0.0021676	−0.93305	−0.014736	0.84446	−0.085484	−1.327	−0.37952	3.9844
b_1	1.5067	3.7346	−0.84452	−6.7793	1.7005	15.8609	3.9936	−64.2103
b_2	–	−1.9223	3.5661	18.7505	−10.1131	−76.3337	−15.4935	443.9398
b_3	–	–	−1.8218	−20.6575	25.0462	188.602	24.2331	−1717.9645
b_4	–	–	–	8.9236	−26.41	−252.2619	−0.79445	4066.5448
b_5	–	–	–	–	10.9548	174.4093	−43.0298	−6026.6841
b_6	–	–	–	–	–	−47.9535	48.9612	5460.8914
b_7	–	–	–	–	–	–	−16.4791	−2765.8366
b_8	–	–	–	–	–	–	–	600.4343

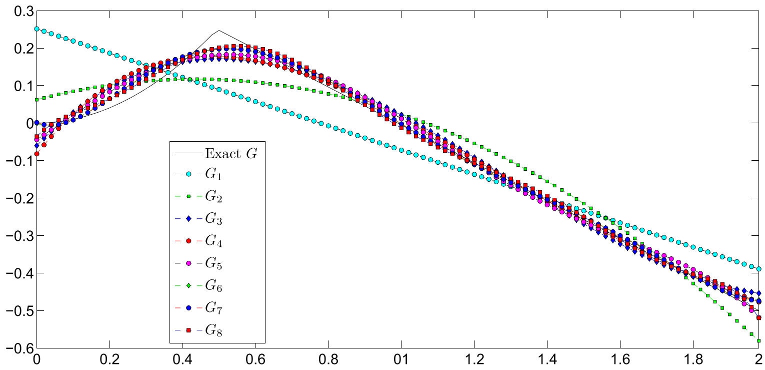

Fig. 5 The analytical and numerical solutions for the boundary function $G(u)$ for the IHCP given by Example 3

($M = N = 512$ and $\varepsilon = 0.0001$). As we expected, the relative l_2 errors and the RMS-norm errors of numerical results was gradually decreased by increasing the mesh points.

Finally Figs. 3 and 4 illustrate the comparison between the exact and the computed solutions for both functions $G(u)$ and $H(u)$ when $M = N = 512$ and $\varepsilon = 0.0001$.

Example 3 As the final test problem consider the problem (1)–(6) with the following assumptions

$$x_1 = 0.65, \ \varphi_1(t) = 2t + \frac{169}{400}, \ \varphi_2(t) = 1.3, \ \gamma(x) = x^2, \ a = 1, \ f(x,t) = 0,$$

$$\psi_1(t) = \begin{cases} -4t^2, & 0 < t < \frac{1}{4} \\ \frac{1}{2}(2t-1), & \frac{1}{4} \le t \end{cases}, \quad \psi_2(t) = \begin{cases} 1-2t, & 0 < t < \frac{1}{2} \\ 2t-1, & \frac{1}{2} \le t \end{cases}.$$

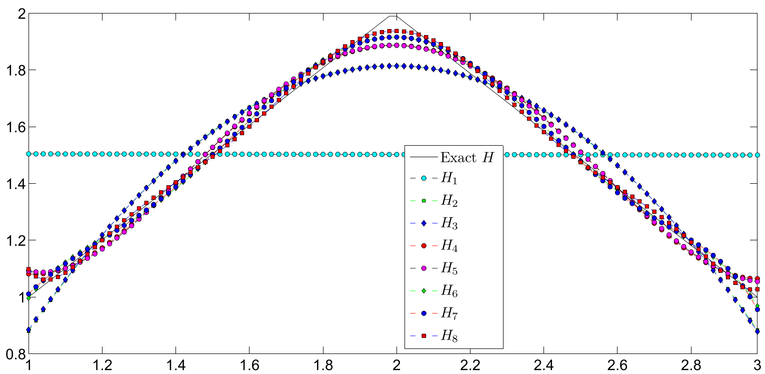

Fig. 6 The analytical and numerical solutions for the boundary function $H(u)$ for the IHCP given by Example 3

The exact solutions for $u(x,t)$, $G(u)$ and $H(u)$ may be derived as

$$u(x,t)=x^2+2t,\ G(u)=\begin{cases} u^2, & 0<u<\frac{1}{2} \\ \frac{1}{2}(1-u), & \frac{1}{2}\le u. \end{cases},\ H(u)=\begin{cases} u, & 0<u<2 \\ 4-u, & 2\le u. \end{cases}.$$

Increasing the degree K of the functions $G_K(u)$ and $H_K(u)$ from 1 to 8, when $\varepsilon = 0.0001,\ 0.001,\ 0.01$ and $M = N = 64,\ 128,\ 256,\ 512$ results in gradual improvement in the accuracy of the relative l_2 errors for computing u, u_x, u_t tabulated in Table 9, the RMS-norm errors between the computed and the exact boundary functions G and H tabulated in Table 10, and the coefficients a_j and $b_j;\ j = 1, 2, ..8$ of the function $G_K(u)$ and $H_K(u)$ tabulated in Tables 11 and 12. Figures 5 and 6 show the comparison between the exact and the computed solutions for both functions $G(u)$ and $H(u)$ when $M = N = 512$ and $\varepsilon = 0.0001$.

6 Conclusion

In this study, a class of inverse heat conduction problems have been investigated with unknown nonlinear boundary conditions. A regularization approach based on the mollification method and the space marching scheme is developed to solve the proposed inverse problem numerically and the missing terms involving the boundary conditions are constructed in the form of a polynomial. The stability and convergence of the solution of the proposed numerical approach are proved and some examples are investigated to support the main results of this work. The theoretical and numerical results presented here validate the use of discrete mollification as a suitable method for determining the boundary condition laws in one-dimensional inverse heat conduction problems. Future work will concern an extension to higher dimensions.

Acknowledgments The authors would like to thank the anonymous referees for their valuable comments and suggestions which substantially improved the manuscript.

References

1. Cannon, J.R.: The one-Dimensional Heat Equation. Addison-Wesley (1984)
2. Özisik, M.N.: Heat Conduction. John Wiley & Sons INC (1993)
3. Saldanha da Gama, R.M.: Simulation of the steady-state energy transfer in rigid bodies, with convective/radiative boundary conditions, employing a minimum principle. J. Comp. Phys. **99**, 310–320 (1992)
4. Wolf, D.H., Incropera, F.P., Viskanta, R.: Jet impingement boiling. Adv. Heat Transf. **23**, 1–132 (1993)
5. Kaiser, T., Troltzsch F: An inverse problem arising in the steel cooling process. Wissenschaftliche Zeitung TU Karl-Marx-Stadt **29**, 212–218 (1987)
6. Beck, J.V., Blackwell, B.: Inverse Heat Conduction: Ill-Posed Problems. Wiley Interscience, New York (1985)
7. Cannon, J.R., Zachman, D.: Parameter Determination in Parabolic Differential equation from overspecified boundary data. Int. J. Eng. Sci. **20**, 779–788 (1982)
8. Rosch, A.: Identification of nonlinear heat transfer laws by optimal control. Numer. Funct. Anal. Optim. **15**, 417–434 (1994)
9. Rosch, A.: Stability estimates for the identification of nonlinear heat laws. Inverse Probl. **12**, 743–756 (1996)

10. Rosch, A.: A Gauss-Newton method for the identification of non-linear heat transfer laws. Int. Ser. Numer. Math **139**, 217–230 (2002)
11. Onyango, T.T.M., Ingham, D.B., Lesnic, D.: Reconstruction of boundary condition laws in heat conduction using the boundary element method. Comput. Math. Appl. **57**, 153–168 (2009)
12. Bialecki, R., Divo, E., Kassab, A.J.: Reconstruction of time-dependent boundary heat flux by a BEM based inverse algorithm. Eng. Anal. Bound. Elem. **30**, 767–773 (2006)
13. Garshasbi, M., Damirchi, J., Reihani, P.: Parameter estimation in an inverse initial-boundary value problem of heat equation. J. Adv. Res. Diff. Equ. **2**, 49–60 (2010)
14. Garshasbi, M., Reihani, P., Dastour, H.: A stable numerical solution of a class of semi-linear Cauchy problems. J. Adv. Res. Dyn. Cont. Sys. **4**, 56–67 (2012)
15. Murio, D.A.: Mollification and space marching. In: Woodbury, K (ed.) Inverse Engineering Handbook. CRC Press (2002)
16. Mejia, C.E., Murio, D.A., Zhan, S.: Some applications of the mollification method. In: Lassonde, M. (ed.) App. Opti. Math Eco., pp. 213–222. Physica-Verlag (2001)
17. Acosta, C.D., Mejia, C.E.: Stabilization of explicit methods for convection diffusion equations by discrete mollification. Comput. Math. Appl. **55**, 368–380 (2008)
18. Acosta, C.D., Mejia, C.E.: Approximate solution of hyperbolic conservation laws by discrete mollification. Appl. Numer. Math. **59**, 2256–2265 (2009)